Detection of road cracks with multiple images

Sylvie Chambon

HAL Id: hal-00878872
https://hal.science/hal-00878872

Submitted on 31 Oct 2013

DETECTION OF ROAD CRACKS WITH MULTIPLE IMAGES

Sylvie CHAMBON

Laboratoire Central des Ponts et Chaussées, LCPC, Nantes, France
chambon@lcpc.fr

Abstract: Extracting the defects of the road pavement in images is difficult and, most of the time, one image is used alone. The difficulties of this task are: illumination changes, objects on the road, artefacts due to the dynamic acquisition. In this work, we try to solve some of these problems by using acquisitions from different points of view. In consequence, we present a new methodology based on these steps : the detection of defects in each image, the matching of the images and the merging of the different extractions. We show the increase in performances and more particularly how the false detections are reduced.

1   INTRODUCTION

In many countries, efforts are spent to reduce errors and increase performances of the automatic (or semi-automatic) evaluation of the quality of the road. This quality depends on numerous characteristics: adherence, texture and defects which include the snatching parts, the repairs and the cracks. We focus on the detection of cracks. Forty years ago, this evaluation was manual: it is expensive, hard, dangerous for the employes, not reproducible and not efficient. Nowadays, the detection of defects is made manually on acquisition of the road images (semi-automatic detection). It is less dangerous than forty years ago, but, it is still expensive, not efficient and not reproducible. In the field of automatic analysis of cracks of the road surface, different kinds of methods have been proposed in the literature and even if they become more and more efficient, we can notice two drawbacks that need to be overcome: the detection presents a lot of false detections and false negatives and they are are dedicated only to the detection of road cracks and they are not able to detect other kind of defects. Consequently, the aim of this work is to present a methodology in order to reduce the number of false detections with fusion of multiple detections on different images of the same piece of road. In the first part of this paper, we introduce a state of the art of detection of road cracks. Then, we describe our methodology by giving details about the acquisition, how the cracks are detected, how the images are matched and finally how all the results are used to give the final answer. The last part shows the results in each step of the methodology before giving conclusions and perspectives.

2   ROAD CRACK DETECTION

In the context of detection with one image, four categories of techniques are identified. The *Threshold* methods are the oldest ones and also the most popular (Acosta et al., 1992). These methods are simple but the results contain a lot of false detections. The methods by *morphology* (tools of mathematical morphology), based on a previous thresholding (Tanaka and Uematsu, 1998), allow to reduce false detections but strongly depend on the set of parameters. The *neuron networks*-based methods have been proposed to alleviate the problems of the two first categories (Kaseko and Ritchie, 1993). However, these methods need a learning phase which is not well appropriate to our task. The *filtering* methods are the most recent and most of them are based on a wavelet decomposition (Subirats et al., 2006) or on partial differential equations (Augereau et al., 2001). We can also notice an auto-correlation method (Lee and Oshima, 1994) and some methods also use the decomposition of

texture (Petrou et al., 1996). In the field of the detection of road cracks with multiple images, a method exploits a stereoscopic acquisition of the scene (Wang and Gong, 2002) and the great advantage is the complementarity of the different acquisitions that helps to validate the detection. We have also noticed that for the estimation of surface deformation, stereo-correlation algorithms have been widely investigated (Sutton et al., 2008). It seems that even small deformations can be characterized by such a system. To resume, the mono-detection has shown its limit (a high percentage of false detections) whereas the multiple detections reveal great advantages (validation, possibility of detecting 3D defects) and are very adapted to our task. Consequently, it seems natural to investigate stereoscopic systems to detect cracks.

3 PROPOSED METHODOLOGY

The four steps of our methodology are:

(1) **Acquisition** of multiple images ;

(2) **Crack detection** in each image ;

(3) **Matching** of the images, i.e. to find the homologous pixels in the images ;

(4) **Fusion** of the results, i.e. to merge the different detections by using the matching results.
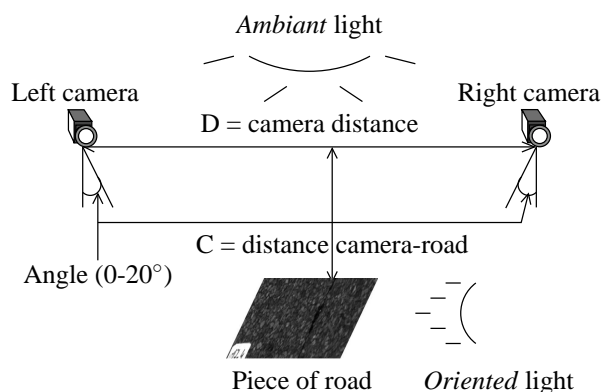

Figure 1: Acquisition system – It is composed of two cameras. The angle of the cameras, the distances between the two sensors, between the sensor and the scene, and the position of the lights are variable. The angle varies from 0 to 20° and the distances between the cameras and between the camera and the scene are adjusted to have good covering between the two images. For the illumination, two options are possible: *ambient* light or *oriented* light.

Acquisition – The quality of the detection results strongly depends on the quality of the acquisition, see Figure 2. Consequently, the choice of the acquisition system is really important for the application and, this is why in the literature, many systems have been proposed and tested. A system is highly dependent on:

- *The type of the sensor* – Three types of sensors can be distinguished: 2D sensors (that need image processing technique), 3D sensors[1] (that are independent from the lighting system) and the merging of 2D sensors and 3D sensors (Fukuhara et al., 1990). We focus on 2D acquisition with cameras.

- *The number of sensors* – Most of the applications use only one sensor or a mosaic of sensors (with no covering between the different acquisitions). (Wang and Gong, 2002) shows that using multiple sensors can improve the performances and, in this paper, we use two cameras.

- *The orientation of the sensor* – It influences the quality of the results. In most of the proposed systems, the camera axis is perpendicular to the road surface and we have tested different orientations: a perpendicular position and an angular position (with 10° and 20°), see Figure 1.

- *The consideration of the illumination changes* – They are one of the main difficulties. For solving it, two possibilities are given: using natural light or controlled light. Without controlled light, it is necessary to pre-process the images for reducing shadows and under/over-lighting areas, whereas, with controlled light, these problems are less influent. However, the lighting system must be designed in order to preserve the crack signal that represents less than 1.5% of the images and is not well contrasted with the road surface (Schmidt, 2003). An other way to solve illumination problem can be by using a stereoscopic system, however, in this work, we added a controlled illumination system in order to study both the contribution of a stereoscopic system and the influence of the type of light (*Ambient* light or *Oriented* light), see Figure 1.

Crack Detection – We use a wavelet decomposition analysis (Chambon et al., 2010) based on two steps: first, to binarize images with a matched filtering and, second, to refine the results with a Markov model-based segmentation, see (Chambon et al., 2010) for more details about the method and Figure 3 for an example. Four variants are tested and compared in this paper: *Init*, the initial work proposed in (Subirats et al., 2006), *Gaus*, a variant that represents the crack by a Gaussian function, *InMM*, the initial version with an improvement of the Markov model-based segmentation (new definition of the sites and of the potential function) and *GaMM*, *Gaus* with the new Markov model, see Figure 3.

---

[1] see http://phnx-sci.com/index.html

(a)

ANGLE	0°	10°	20°
Ambient			
Oriented			

(b)

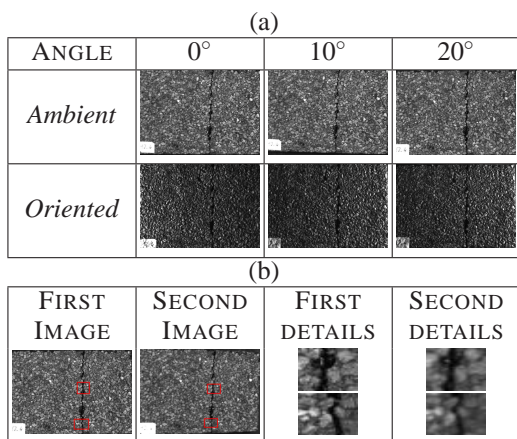| FIRST IMAGE	SECOND IMAGE	FIRST DETAILS	SECOND DETAILS

Figure 2: Acquisition conditions, see Figure 1 for the details about the acquisition system – We can see the same piece of road which is acquired with the 6 different possibilities in (a). Visually, it seems that the crack is better contrasted with *Ambient* illumination than with *Oriented* illumination. The images in (b) give an illustration of the differences between two images of a stereoscopic pair. In the right part, it represents the details of the red areas in the left part.

Matching – The goal of this step is to find correspondent pixels in the two images, i.e. pixels that represent the same point of the scene. We consider $\mathbf{p}_{i,j}^1$ the pixel in the first image and $\mathbf{p}_{k,l}^2$ its homologous pixel in the second image. A lot of algorithms have been proposed for stereoscopic matching. We can distinguish two kinds of methods: local ones, based on a local similarity cost optimized with a winner take all strategy, and global ones where a global cost on all the correspondent pairs of pixels is optimized (Scharstein and Szeliski, 2002). We work with high-textured images with no occlusion and it seems quite natural to work with a local method. A correlation measure is used and it evaluates how two sets of data are similar, i.e. the grey levels of the two pixels and their neighborhoods (which are contained in a correlation window). We have studied the advantages of correlation measures and we decided to try five of them (the best ones in our previous evaluation): the well known Normalized Cross Correlation (NCC) which uses a scalar product ; the Sum of Absolute Differences (SAD) ; the Gradient Correlation (GC) based on the derivatives of the images ; the RANK measure which evaluates the dissimilarity between the rank of the data, i.e. the grey levels in the correlation window (Zabih and Woodfill, 1994) ; and finally, the Smooth Median Absolute Deviation (SMAD) which evaluates the sum of the h^2 first squared differences between the two correlation win-

_____
[2]Here, h is half of the size of the correlation window.

dows. For more details on the correlation measures see (Chambon and Crouzil, 2003). The matching algorithm is explained in Figure 4. Moreover, we add a symmetric constraint: matching is done from the first image to the second and from the second to the first and all correspondences that are not coherent are removed, i.e. the pixels are considered as unmatched or undetermined. The results are presented in section 4.
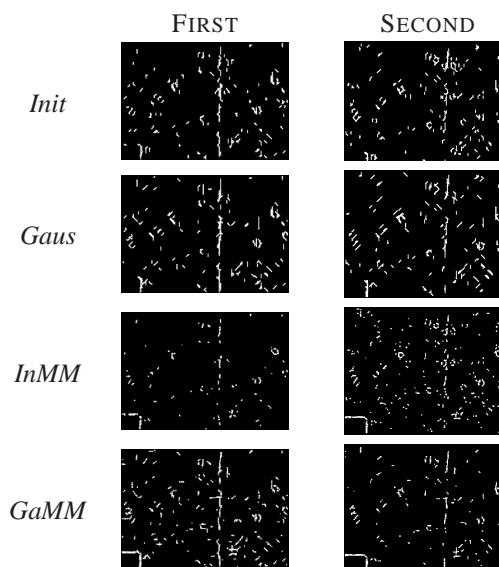
FIRST	SECOND

Figure 3: Crack detection – Examples of the results of the four variants on one image, see image with 10° and *ambient* light in Figure 2. White pixels correspond to pixels considered as a crack. The *Init* and *Gaus* methods show a quite dense detection, with a lot of false detections, whereas, the two others are more sparse but with less false detections. A quantitative analysis is given in section 4. For each variant, it illustrates how the results are complementary.

$$M(\mathbf{f}_{i,j}^1, \mathbf{f}_{k,l}^2) \qquad \text{ROI}(\mathbf{p}_{i,j}^1)$$
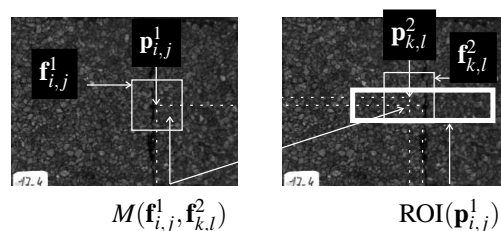
Figure 4: Matching algorithm – For each pixel $\mathbf{p}_{i,j}^1$ in the first image, a region of interest, $\text{ROI}(\mathbf{p}_{i,j}^1)$, is determined in the second image. It corresponds to all the potential correspondent pixels. For each pixel of $\text{ROI}(\mathbf{p}_{i,j}^1)$, $\mathbf{p}_{k,l}^2$, a similarity score or correlation score, M, is evaluated between the grey levels of the pixels in their respective neighborhoods, $\mathbf{f}_{i,j}^1$ and $\mathbf{f}_{k,l}^2$, also called the correlation windows. The pixel $\mathbf{p}^2 = \text{argmax}_{k,l} M(\mathbf{f}_{i,j}^1, \mathbf{f}_{k,l}^2)$ (i.e. that obtains the best score) is considered as the correspondent pixel of $\mathbf{p}_{i,j}^1$.

Fusion – We define the label function l that equals 0 when a pixel $\mathbf{p}$ is labelled as background and 1 when it is a crack. We also introduce the disparity function d which equals the distance between a pixel and its correspondent. This function equals -1 when no match has been found. We propose an algorithm to merge the results of matching and the two crack detections based on two steps:

1. *Initialization step* – Each pixel $\mathbf{p}_{i,j}$ that obtains the same label in the two views is validated whereas the others are not, i.e.:

   if $((l(\mathbf{p}_{i,j}^1) = l(\mathbf{p}_{k,l}^2)) \ \& \ (d(\mathbf{p}_{i,j}^1) \neq -1))$

   then $l(\mathbf{p}_{i,j})$ is validated.

   else $l(\mathbf{p}_{i,j})$ is considered as undetermined.

2. *Iterative step* – The aims are to fill the undetermined pixels and to add some points when there are near pixels considered as crack. We use the hypothesis that a crack is composed of a set of connected segments with different orientations. Consequently, we build a map of vote by estimating the cost of each path from the studied pixel to the eight possible directions. More formally, while the labels change:

   For each validated pixels, we estimate a vote map (local map), noted V, in a centered squared neighborhood of size $2s + 1$[3]:

   $$\forall \mathbf{p}_{m,n} \in \mathcal{V}(\mathbf{p}_{i,j}), V(\mathbf{p}_{m,n}) = \sum_{k=0}^{s} c(\mathbf{p}_{i+km,j+kn}) \quad (1)$$

   where $\mathcal{V}(\mathbf{p}_{i,j})$ is the set of the 8 neighbors of $\mathbf{p}_{i,j}$ and (m,n) corresponds to one of the 8 possible directions and c is defined by:

   $$c(\mathbf{p}_{i,j}) = \begin{cases} 1 & \text{if } l(\mathbf{p}_{i,j}) = 1 \\ 0 & \text{otherwise} \end{cases} \quad (2)$$

   We select $\mathbf{p}_d$ defined by:

   $$\mathbf{p}_d = \underset{\mathbf{p}_{m,n}}{\operatorname{argmax}}(V(\mathbf{p}_{m,n})), \quad (3)$$

   and finally:

   $$l(\mathbf{p}_d) = 1$$
   $$\forall \mathbf{p} \in \mathcal{V}(\mathbf{p}_{i,j}) \text{ with } \mathbf{p} \neq \mathbf{p}_d, l(\mathbf{p}_{m,n}) = 0. \quad (4)$$

3. *Final step* – At the end of the process, each undetermined pixel is marked as background.

4 EXPERIMENTAL RESULTS

Evaluation Setup – We have tested 29 stereoscopic acquisitions of the same piece of road. These images

---

[3]In our experiments, the size of s equals the size of the correlation window used for matching

have been manually segmented and we use this manual segmentation as a reference for quantitative evaluation. For the detection, we evaluate the percentages of: True Positives (TP), Accepted detections (ACC, they correspond to pixels distant from 1 pixel from the manual segmentation), False Positives (FP), False negatives (FN). We also estimate the similarity coefficient, or DICE, which is equals to: $\frac{2TP}{FN+P+FP}$. In each part of the analysis, we link the quality of the results with the kind of acquisition.

Table 1: Detection results – These values are the mean results obtained for the images with the best illumination conditions, i.e. the *ambient* illumination.

METHOD	IMAGE	TP	ACC	FP	FN	DICE
Init	First	10.41	22.81	66.78	16.30	**0.51**
	Second	7.17	18.39	74.45	32.93	0.41
Gaus	First	**11.40**	20.85	67.65	15.78	0.50
	Second	7.14	17.72	75.14	32.21	0.40
InMM	First	11.17	**25.43**	63.4	47.99	0.49
	Second	5.93	18.04	76.02	37.26	0.41
GaMM	First	8.86	21.05	70.09	**12.81**	0.49
	Second	8.22	23.72	68.06	40.87	0.46

Analysis of the detection It clearly appears that for all the criteria, an *Ambient* light always permits to obtain the best results, in particular, with an angle of $20°$. Table 1 shows the mean values of the criteria for all the images with this illumination configuration. It shows that results are different between the first view and the second view and that the results in the both views can be improved. A visual result is also presented in Figure 3.

Matching results – We evaluate the quality of the results with the density of the response (the percentage of pixels that are matched) and the execution time, with different correlation window sizes, see Figure 5. RANK obtains the best density and the best execution time. With a window size lower than 9×9, results are quite bad and when the size is greater than 15×15 the density is not really improved (it highlights known phenomenons). Visual results are presented with disparity maps[4], see Figure 6. The maps of RANK and GC are the clearest ones, i.e. that present less false negatives (black pixels). It also shows that SAD and SMAD seem less sensitive to the difficulties in the large black area on the bottom of the crack.

---

[4]For each pixel, it gives the distance between the considered pixel and its correspondent: the clearer the pixel, the larger the distance. Black pixels are unmatched pixels.
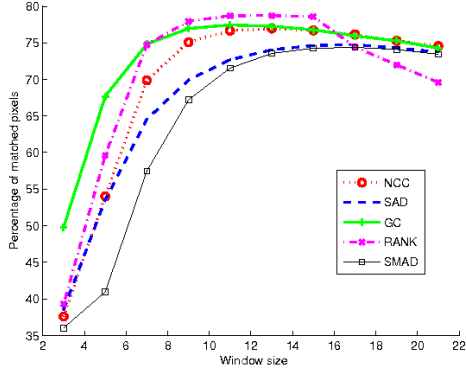
EXECUTION TIME (in seconds for 9×9 window)

NCC	SAD	GC	RANK	SMAD
121.1	156.7	1033.72	91.52	1410.38

Figure 5: Density of matching and execution time – We have estimated the disparities between the two images with different sizes of correlation window. It appears that RANK, GC and NCC obtain good density. The maximum is reached between 9×9 and 11×11. All the results given are the mean of the results obtained with the 29 couples.

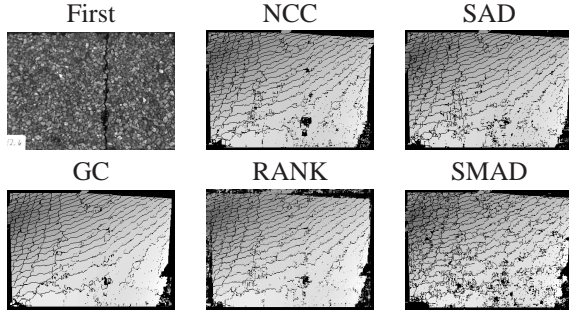| First	NCC	SAD
GC	RANK	SMAD

Figure 6: Disparity maps – It shows typical results obtained with this kind of images. Main problems are due to large non-textured regions that correspond, in this case, to some parts of the crack.

Fusion results – The results of the fusion have been quantitatively analyzed, see Table 2. The percentage of good or accepted detections are higher than those obtained with only one image whereas the percentage of false negatives is higher and consequently, the DICE values are sometimes not better than the initial ones. The important aspect is that, as expected, we have increased the reliability of the result but the results are sparser. The percentage of TP+ACC is always improved, for each possible measure and each possible detection method. The increase in performances varies from 8 points to 22 points. In these results, PD (Percentage Difference between the per-

centage of the correct detections in one image and the percentage correct detections with the fusion of the two detections) is always negative and means that the fusion outperforms the initial results. In conclusion, the reliability of the detection is higher whereas the crack is less detected. The second analysis is that GC, RANK and SMAD obtain better results than those given by classic measures and it confirms that we need a window size larger enough (more than 11×11) to obtain reliable correspondences. Finally, it seems that the *Gaus* method allows to obtain the most complementary results. An illustration of the results is given in Figure 7. The detection maps given are clearer than the ones given in Figure 3 but they are also sparser.

Table 2: Fusion results – For each measure (MEA.), we notice the window size (WIN.) that permits to obtain the best value of DICE. In brackets, we precise the differences between the percentage of TP+ACC obtained with each image alone and with the fusion of the two results. The bold letters indicate the best results for each criterion and the italic letters illustrate when the DICE is better than using just one image. PD is explained in § "Fusion result".

MEA.	WIN.	TP+ACC	FP	FN	PD	DICE
		Init				
NCC	19	45.6 (12.4)	54.4	70.1	-14.2	0.42
SAD	13	48.6 (15.4)	51.4	69.8	-13.2	0.43
GC	13	47 (13.7)	53	54.1	-6.3	*0.54*
RANK	15	47.2 (14)	52.8	52.1	-5.2	*0.55*
SMAD	19	49 (15.8)	51	53.2	-4.9	*0.55*
		Gaus				
NCC	9	54.3 (22)	45.7	70.8	-11.5	0.43
SAD	9	**55.1** (22.8)	44.8	69.2	-10.3	0.45
GC	11	48.1 (15.7)	51.9	**49.2**	-2.9	**0.57**
RANK	15	48 (15.7)	52	52.5	-4.5	*0.55*
SMAD	19	49.4 (17.1)	50.6	54.2	-4.7	*0.54*
		InMM				
NCC	7	50.7 (14)	49.4	75.6	-6.7	0.38
SAD	11	52 (15.2)	48	73.3	-5.2	0.4
GC	21	41.5 (4.8)	58.5	67.2	-5.5	0.44
RANK	21	43.5 (6.8)	56.5	66.4	-4.5	0.45
SMAD	13	43.4 (6.7)	56.6	65	-3.9	0.46
		GaMM				
NCC	9	50.2 (20.2)	49.9	70.1	-11.1	0.42
SAD	11	48.1 (18.1)	51.9	70.7	-12	0.42
GC	13	38.2 (8.3)	61.8	59.9	-10.8	0.47
RANK	15	39.1 (9.2)	60.9	58.6	-9.9	0.48
SMAD	13	42 (12)	58	60.4	-9.5	0.48

5 CONCLUSION

In the field of the detection of road cracks, we proposed an original methodology based on a stereoscopic system. Our contributions concern the propo-

sition of the generic algorithm, the study of the influence of different illumination conditions, the introduction of different kind of correlation measures for the matching step and how all the results are merged. The results are quite encouraging and they highlight the best conditions: acquisition with ambient illumination, detection with the method that considers the crack as a Gaussian function and matching with a correlation measure based on the gradients of the image. Even if we have a specific application, i.e. crack detection, this method can be used to detect other types of defects in other type of difficult objects (low contrasted defects in highly textured objects). This work can be improved and future work will introduce a more systematic study of the influence of the light position using (Drbohlav and Chantler, 2005). The matching step will be evaluated quantitatively and the tested images will be completed (with natural images and different kind of textures). Finally, the 3D reconstruction step will be added to complete the crack detection and include other defect detection, like the snatching of pieces of road.
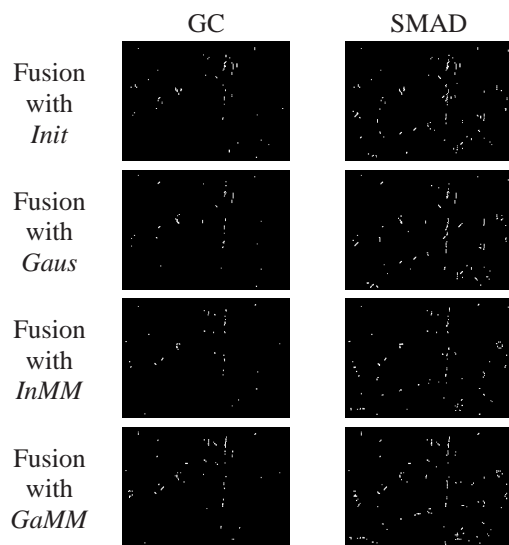

Figure 7: Detection maps with fusion method – Results are shown for the same image as the results in Figure 3 and only for two of the best correlation measures and for each detection methods studied. It illustrates that the best performances are reached with the *Gaus* detection method combined with a GC matching.

REFERENCES

Acosta, J., Adolfo, L., and Mullen, R. (1992). Low-Cost Video Image Processing System for Evaluating Pavement Surface Distress. *TRR: Journal of the Transportation Research Board*, 1348:63–72.

Augereau, B., Tremblais, B., Khoudeir, M., and Legeay, V. (2001). A Differential Approach for Fissures Detection on Road Surface Images. In *International Conference on Quality Control by Artificial Vision*.

Chambon, S. and Crouzil, A. (2003). Dense matching using correlation: new measures that are robust near occlusions. In *BMVC*.

Chambon, S., Gourraud, C., Moliard, J.-M., and Nicolle, P. (2010). Road crack extraction with adapted filtering and markov model-based segmentation. In *VISAPP*.

Drbohlav, O. and Chantler, M. (2005). On optimal light configurations in photometric stereo. In *ICCV*, pages 1707–1712.

Fukuhara, T., Terada, K., Nagao, M., Kasahara, A., and Ichihashi, S. (1990). Automatic pavement-distress-survey system. *ASCE, Journal of Transportation Engineering*, 116(3):280–286.

Kaseko, M. and Ritchie, S. (1993). A neural network-based methodology for pavement crack detection and classification. *Transportation Research Part C: Emerging Technologies information*, 1(1):275–291.

Lee, H. and Oshima, H. (1994). New Crack-Imaging Procedure Using Spatial Autocorrelation Function. *ASCE, Journal of Transportation Engineering*, 120(2):206–228.

Petrou, M., Kittler, J., and Song, K. (1996). Automatic surface crack detection on textured materials. *Journal of Materials Processing Technology*, 56(1–4):158–167.

Scharstein, D. and Szeliski, R. (2002). A Taxomomy and Evaluation of Dense Two-Frame Stereo Correspondence Algorithms. *IJCV*, 47(1):7–42.

Schmidt, B. (2003). Automated pavement cracking assessment equipment – State of the art. Technical Report 320, Surface Characteristics Technical Committee of the World Road Association (PIARC).

Subirats, P., Fabre, O., Dumoulin, J., Legeay, V., and Barba, D. (2006). Automation of pavement surface crack detection with a matched filtering to define the mother wavelet function used. In *EUSIPCO*.

Sutton, M., Yan, J., Tiwari, V., Schreier, H., and Orteu, J. (2008). The effect of out-of-plane motion on 2D and 3D digital image correlation measurements. *Optics and Lasers in Engineering*, 46:746–757.

Tanaka, N. and Uematsu, K. (1998). A Crack Detection Method in Road Surface Images Using Morphology. In *Workshop on Machine Vision Applications*, pages 154–157.

Wang, K. and Gong, W. (2002). Automated Pavement Distress Survey: A Review and A New Direction. In *Pavement Evaluation Conference*, pages 21–25.

Zabih, R. and Woodfill, J. (1994). Non-parametric Local Transforms for Computing Visual Correspondence. In *ECCV*, pages 151–158.